Available online at www.sciencedirect.com

ScienceDirect

Structural Integrity Procedia 00 (2021) 000–000

Structural Integrity Procedia

www.elsevier.com/locate/procedia

5th International Conference on Structural Integrity and Durability

On the predictive capability of stress-based multiaxial high-cycle fatigue criteria

T.L. Castro[a,*], T.A. Peixoto[a], B. Carvalho[a], M.V. Pereira[a], F.A. Darwish[b]

[a]*Pontifical Catholic University of Rio de Janeiro, Department of Chemical and Materials Engineering, Rua Marquês de São Vicente 225, Rio de Janeiro, 22451-900, RJ, Brazil*

[b]*Fluminense Federal University, Department of Civil Engineering, Rua Passo da Pátria 156, Niterói, 24210-240, RJ, Brazil*

Abstract

Six multiaxial fatigue models, namely Matake (M), Findley (F), Susmel & Lazzarin (S&L), Carpinteri & Spagnoli (C&S), Liu & Mahadevan (L&M) and Papadopoulos (P), were selected and compared in their predictive capability relative to 65 critical loading conditions. Given that the left-hand side (LHS) of the expressions is associated to the driving force to failure while the right-hand side (RHS) is associated to fatigue resistance, critical loading conditions should drive the criteria to yield a relative difference between LHS and RHS approaching zero. Accordingly, positive I values indicate failure, while negative I values indicate that the component should be able to withstand the given loading condition. The results of the 65 error indices for each model is presented in the form of histograms and analysed in terms of dispersion range, overall average and percentual frequency within a central range between ±10%. It was observed that Papadopoulos' criterion presented the smallest dispersion and best overall average.

Keywords: fatigue behaviour; fatigue-life prediction; mesoscopic scale-based model; sinchronous sinusoidal bending and torsion; error indices

1. Main text

A large number of multiaxial high cycle fatigue damage criteria have been introduced over many decades, aiming at predicting fatigue failure of metallic materials under time-varying multiaxial stresses. Several reviews of popularly

* Corresponding author. Tel.: +55 21 988586220.
E-mail address: tiagocastrobl@gmail.com

used criteria can be found in the literature, as in Y. S. Garud (1981), You and Lee (1996), Papadopoulos *et al.* (1997), Carpinteri and Spagnoli (2001) and Wang and Yao (2004), where one can verify that critical plane-based models represent an important group for high-cycle fatigue analysis. Application of such models depends in the first place on prior identification of the critical plane where fatigue damage can occur leading to crack initiation and one can thus proceed to calculate the stresses acting on the plan as a result of the applied cyclic loads.

The present work has the purpose of comparing the capabilities of a number of critical plane-based criteria to predict high cycle fatigue behavior of hard metallic materials under combined bending and torsion. The loading conditions, to which the criteria were applied, were taken from published experimental fatigue resistance limit tests involving synchronous sinusoidal in-phase and out-of-phase loadings. The inequalities representative of five selected models, namely **M** - Matake (1977), **S&L** - Susmel & Lazzarin (2002) , **F** - Findley (1959), **C&S** - Carpinteri & Spagnoli (2001) and **L&M** - Liu & Mahadevan (2005) are respectively given by expressions 1 to 5

$$C_a + \mu N_{max} \leq t_{-1} \tag{1}$$

$$C_a + k' \frac{N_{max}}{C_a} \leq t_{-1} \tag{2}$$

$$C_a + k\, N_{max} \leq f* \tag{3}$$

$$\sqrt{N_{max}^2 + \left(\frac{f_{-1}}{t_{-1}}\right)^2 C_a^2} \leq f_{-1} \tag{4}$$

$$\sqrt{\left[\frac{N_a\left(1+\eta\frac{N_m}{f_{-1}}\right)}{f_{-1}}\right]^2 + \left(\frac{C_a}{t_{-1}}\right)^2} \leq \lambda, \tag{5}$$

where C_a and N_a are, respectively, the shear stress and normal stress amplitudes acting on the critical plane. N_m is the mean normal stress acting on the same plane, and therefore $N_{max} = N_a + N_m$. The constants μ, k', k, $f*$, η and λ are material parameters that are exclusively dependent on fatigue resistance limits, as shown in Table 1.

In addition to the models presented above, a modified version of the C&S criterion, Carpinteri et al. (2013), is also included in the present study. Such version is obtained by replacing N_{max} in expression 4 by the parameter $N_{a,eq}$ given by expression 6, where σ_u is the ultimate strength.

$$N_{a,eq} = N_a + f_{-1}\left(\frac{N_m}{\sigma_u}\right) \tag{6}$$

At this point, it is important to mention that the above given criteria are applicable to hard metallic materials where the ratio t_{-1}/f_{-1} is limited to the range $1/\sqrt{3} \leq t_{-1}/f_{-1} \leq 1$, as described in Carpinteri & Spagnoli (2001). One should also point out that the left-hand side (LHS) of the inequalities refers to the driving force for fatigue failure due to stresses acting on the critical plane. The right-hand side (RHS), on the other hand, is related to the fatigue resistance of the material, hence the comparison between the two sides could indicate whether fatigue failure is likely to happen.

Table 1. Definition of pertinent material constants.

$\mu = 2\left(\frac{t_{-1}}{f_{-1}}\right) - 1$	$k' = t_{-1} - \frac{f_{-1}}{2}$	$k = \frac{2-\left(\frac{f_{-1}}{t_{-1}}\right)}{2\sqrt{\left(\frac{f_{-1}}{t_{-1}}-1\right)}}$	$f* = \sqrt{\frac{f_{-1}^2}{4\left(\frac{f_{-1}}{t_{-1}}-1\right)}}$	$\eta = \frac{3}{4} + \frac{1}{4}\left(\frac{\sqrt{3}-\frac{f_{-1}}{t_{-1}}}{\sqrt{3}-1}\right)$	$\lambda = [\cos^2(2\delta)\, s^2 + \sin^2(2\delta)]^{1/2}$

δ is given by expressions (7) and (8) for the C&S and L&M models, respectively.

2. Critical-plane stresses

For the Matake (1977) and S&L (2002) criteria, the critical plane is defined as the plane on which the shear stress amplitude C_a attains its maximum. For the Findley (1959) criterion, the critical plane is determined by maximizing the linear combination of the shear stress amplitude C_a and the maximum value of the normal stress N_{max}.

As to the C&S - Carpinteri & Spagnoli (2001, 2013) and L&M - Liu & Mahadevan (2005) criteria, the critical plane determination depends on the fracture plane as well as the angle between the two planes, δ. The fracture plane is defined as the plane on which the maximum principal stress N_{max} achieves its greatest value in the course of cyclic loading. Considering that $s = t_{-1}/f_{-1}$, the angle δ for C&S and L&M is respectively given by

$$\delta = \left[1 - \left(\frac{t_{-1}}{f_{-1}}\right)^2\right]\frac{3\pi}{8} \tag{7}$$

$$\delta = \frac{1}{2}cos^{-1}\left[\frac{-2+\sqrt{4-4\left(\frac{1}{s^2}-3\right)\left(5-\frac{1}{s^2}-4s^2\right)}}{2\left(5-\frac{1}{s^2}-4s^2\right)}\right]. \tag{8}$$

Identification of the critical plane and calculation of the stresses acting on it are summarized here for the case of synchronous sinusoidal normal and shear stress loading (Fig. 1), defined by the parameters σ_a, τ_a, σ_m ,τ_m and β, where σ_a and τ_a are respectively the applied normal and shear stress amplitudes, σ_m and τ_m are the corresponding mean stresses and β is the phase difference between the bend and torsion stress components. Fig. 2 shows a general material plane Δ, which is perpendicular to the $x - y$ plane, with its orientation uniquely defined by the angle φ or, equivalently, by its complementary ψ. N_m and N_a acting on Δ are given expressions by 9 to 12, Castro et al. (2021).

$$N_m = sin^2(\theta)\,[\sigma_m\,sin^2(\varphi) + \tau_m\,sin(2\varphi)] \tag{9}$$

$$N_a = \sqrt{a^2 + b^2} \tag{10}$$

$$a = sin^2(\theta)[\sigma_a\,sin^2(\varphi) + \tau_a\,cos(\beta)\,sin(2\varphi)] \tag{11}$$

$$b = -\,sin^2(\theta)\,[\tau_a\,sin(\beta)\,sin(2\varphi)] \tag{12}$$

The shear stress amplitude acting on Δ is given by expression 13 to 17, where $\theta = \pi/2$, (Castro et al., 2021).

$$C_a = \sqrt{\frac{f^2+g^2+p^2+q^2}{2} + \sqrt{\left(\frac{f^2+g^2+p^2+q^2}{2}\right)^2 - (fq - gp)^2}} \tag{13}$$

$$f = \frac{1}{2}sin(2\theta)\,[\sigma_a\,sin^2(\varphi) + \tau_a\,cos(\beta)\,sin(2\varphi)] \tag{14}$$

$$g = -\frac{1}{2}sin(2\theta)\,\tau_a\;sin(\beta)\,sin(2\varphi) \tag{15}$$

$$p = sin(\theta)\left[\frac{1}{2}\sigma_a\,sin(2\varphi) + \tau_a\,cos(2\varphi)\,cos(\beta)\right] \tag{16}$$

$$q = -\,sin(\theta)\,\tau_a\,sin(\beta)\,cos(2\varphi) \tag{17}$$

By maximizing C_a with respect to the angle φ by varying φ according to an increment of 0.1°, one can determine the critical plane orientation φ_c as well as the corresponding C_a, N_a and N_m values. Both the Matake and S&L criteria can thus be applied by substituting the values obtained for a given loading condition in the LHS of expressions 1 and

2. The same procedure is also valid for applying the Findley criterion, except for the fact that, instead of maximizing C_a, the LHS of expression 3 is to be maximized with respect to φ and the maximum value thus obtained is to be compared to the RHS of the same expression.

The fracture plane orientation, defined by φ_f as shown in Fig. 3, is determined by maximizing N_{max} with respect to φ and hence the critical plane orientation φ_c for both C&S and L&M criteria will be given by $\varphi_c = \varphi_f - \delta$, or equivalently by $\psi_c = \psi_f + \delta$.

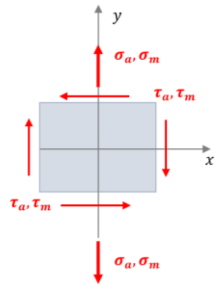

Fig. 1. Plane stress loading conditions.

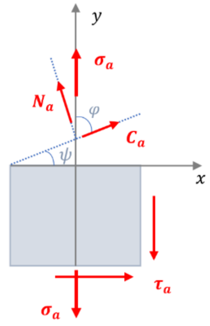

Fig. 2. General material plane normal to the $x - y$ plane with its orientation defined by the angle φ or by its complementary ψ.

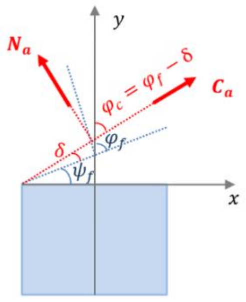

Fig. 3. Critical plane orientation φ_c and its relation to fracture plane orientation φ_f in the C&S and L&M criteria

Knowing φ_c for each criterion, C_a, N_a and N_m values can be calculated and substituted in the LHS of the corresponding inequalities, which is then to be compared with the RHS. The error index I, which refers to the relative difference between the two sides, can be estimated as

$$I = \frac{LHS - RHS}{RHS} \times 100. \tag{18}$$

With the error index I tending to zero, a given criterion is considered to be in good agreement with the experiment carried out for a set of cyclic bending and torsion. Positive I values, on the one hand, are indicative of fatigue failure in a situation where failure is not observed, and the criterion is considered to be conservative. Negative I values, on the other hand, indicate that a selected criterion is non-conservative, as it may permit an increase in the applied cyclic loads, thus leading to higher risk of fatigue failure.

3. Applying the models

In order to evaluate their predictive capabilities, the selected critical plane-based criteria were applied to a number of cyclic bend and torsion loadings of six different metallic materials, presented by Zenner et al. (1985), Nishihara & Kawamoto (1945) and Froustey & Lasserre (1989). The loading parameters are reported in Table 2, together with the materials' pertinent mechanical characteristics.

Table 2. Critical loading conditions, total of 65, relative to 6 different materials

Material		f-1 (MPa)	t-1 (MPa)	σ_u (MPa)
Swedish hard steel		313,9	196,2	704,1
σ_a(MPa)	σ_m(MPa)	τ_a(MPa)	τ_m(MPa)	β(°)
327,7	0	0	0	0
308	0	63,9	0	0
255,1	0	127,5	0	0
141,9	0	171,3	0	0
0	0	201,1	0	0
255,1	0	127,5	0	30
142	0	171,2	0	30
255,1	0	127,5	0	60
147,2	0	177,6	0	60
308	0	63,9	0	90
264,9	0	132,4	0	90
152,5	0	184,2	0	90

2(a) - Swedish hard steel

Material		f-1 (MPa)	t-1 (MPa)	σ_u (MPa)
Hard steel		313,9	196,2	680
σ_a(MPa)	σ_m(MPa)	τ_a(MPa)	τ_m(MPa)	β(°)
138,1	0	167,1	0	0
140,4	0	169,9	0	30
145,7	0	176,3	0	60
150,2	0	181,7	0	90
245,3	0	122,7	0	0
249,7	0	124,9	0	30
252,4	0	126,2	0	60
258	0	129	0	90
299,1	0	62,8	0	0
304,5	0	63,9	0	90

2(b) - Hard steel

Material		f-1 (MPa)	t-1 (MPa)	σ_u (MPa)
42CrMo4		398	260	1025
σ_a(MPa)	σ_m(MPa)	τ_a(MPa)	τ_m(MPa)	β(°)
328	0	157	0	0
286	0	137	0	90
233	0	224	0	0
213	0	205	0	90
266	0	128	128	0
283	0	136	136	90
333	0	160	160	180
280	280	134	0	0
271	271	130	0	90

2(c) - 42CrMo4

Material		f-1 (MPa)	t-1 (MPa)	σu (MPa)
34Cr4		410	256	795
σa(MPa)	σm(MPa)	τa(MPa)	τm(MPa)	β(°)
314	0	157	0	0
315	0	158	0	60
316	0	158	0	90
315	0	158	0	120
224	0	224	0	90
380	0	95	0	90
316	0	158	158	0
314	0	157	157	60
315	0	158	158	90
279	279	140	0	0
284	284	142	0	90
355	0	89	178	0
212	212	212	0	90
129	0	258	0	90

2(d) - 34Cr4

Material		f-1 (MPa)	t-1 (MPa)	σu (MPa)
30NCD16		660	410	1880
σa(MPa)	σm(MPa)	τa(MPa)	τm(MPa)	β(°)
485	0	280	0	0
480	0	277	0	90
480	300	277	0	0
480	300	277	0	45
470	300	270	0	60
473	300	273	0	90
590	300	148	0	0
565	300	141	0	45
540	300	135	0	90
211	300	365	0	0

2(e) - 30NCD16

Material		f-1 (MPa)	t-1 (MPa)	σu (MPa)
Mild steel		235,4	137,3	518,8
σa(MPa)	σm(MPa)	τa(MPa)	τm(MPa)	β(°)
245,3	0	0	0	0
235,6	0	48,9	0	0
187,3	0	93,6	0	0
101,3	0	122,3	0	0
0	0	142,3	0	0
194,2	0	97,1	0	60
108,9	0	131,5	0	60
235,6	0	48,9	0	90
208,1	0	104,1	0	90
112,6	0	136	0	90

2(f) - Mild steel

The results obtained are presented in Fig. 4, in the form of frequency histograms of the error index I. This figure is comprised of graphs corresponding to the M, F, C&S, Modified C&S, L&M and S&L criteria. The abscissa represents the values of the error index I, divided in intervals of 5%. The column drawn above each interval corresponding to the frequency, i.e., the number of loading conditions whose I values pertain to the given interval.

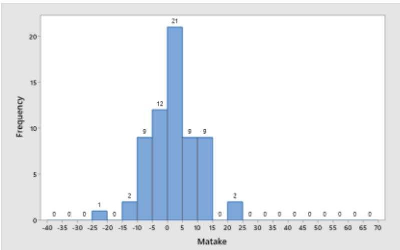

Fig. 4(a) - Matake

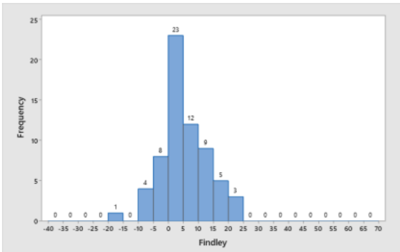

Fig. 4(b) - Findley

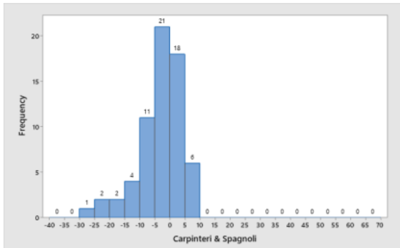

Fig. 4(c) – C&S

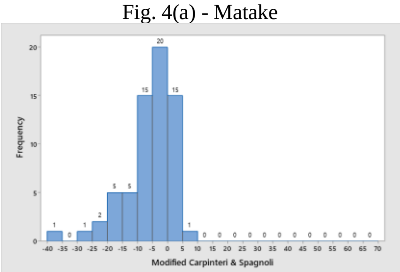

Fig. 4(d) – Modified C&S

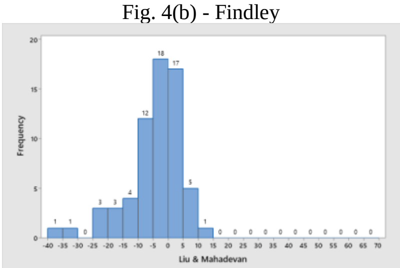

Fig. 4(e) – L&M

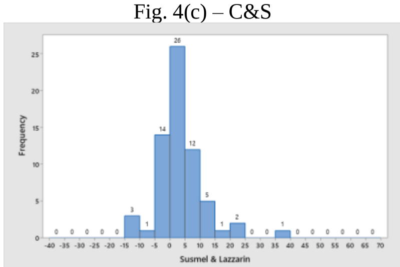

Fig. 4(f) – S&L

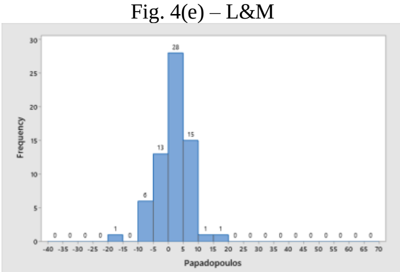

Fig. 4(g) – Papadopoulos

Fig. 4. Frequency histograms depicting the error index dispersion values for the criteria in question.

Fig. 4 also includes a seventh graph, which depicts the frequency histogram of the I values associated with applying a mesoscopic scale-based model, developed by Papadopoulos *et al.* (1997), to the same loading conditions. The inequality representative of this model is expressed as

$$\sqrt{\left(\frac{\sigma_a^2}{3}+\tau_a^2\right)}+\alpha\left(\frac{\sigma_a+\sigma_m}{3}\right)\leq t_{-1}, \tag{19}$$

where

$$\alpha=\left(\frac{3\,t_{-1}}{f_{-1}}\right)-\sqrt{3}. \tag{20}$$

An important advantage of the Papadopoulos model refers to the fact that it is independent of critical plane, but it is also to be remembered that its validity is restricted to materials for which range $1/\sqrt{3}\leq\ t_{-1}/f_{-1}\leq 0.8$ (Papadopoulos et al., 1997).

3.1. Discussing the error index

Examining the histograms shown in Fig. 4, one can conclude that the predictions made by the criteria in question exhibit different degrees of dispersion. As listed in Table 3, the error index I varies from -38% to 10% for the L&M criterion, indicating a dispersion range of 48%. In a decreasing order, this is followed by a dispersion of 47%, 45%, 41%, 38% e 36% for the S&L, M, Modified C&S, F and C&S criteria, respectively. As to the Papadopoulos criterion, an error index dispersion of 32% is noticeable.

Table 3. Frequency histogram deviations.

	Average	Std deviation	Min	Median	Max	Amplitude
Matake, M	2.45	7.99	-21.65	2.85	24.02	45.67
Findley, F	5.30	7.49	-16.13	4.40	22.41	38.54
Carpinteri & Spagnoli, C&S	-2.84	7.40	-26.81	-1.56	8.78	35.59
Modified C&S	-5.66	8.26	-35.96	-3.58	5.90	41.86
Liu & Mahadevan, L&M	-4.36	9.30	-38.55	-2.66	10.29	48.84
Papadopoulos, P	1.80	5.27	-15.34	2.50	16.68	32.02
Susmel & Lazzarin, S&L	3.64	7.53	-12.51	2.90	35.15	47.66

Table 3 also indicates that, among all of the criteria in question, the Papadopoulos criterion displays the lowest error index average value (situated at 1.8%), with lowest standard deviation (5.2%). However, a low average value of I is not a definite indication of good predictive capability as positive values cancel out with negative ones.

An effective method of evaluating the efficacy of a given criterion is to determine the number of tests (loading conditions) which belong to a selected I interval around zero, for example from -10% to 10%. The closer this number to the total number of tests, the higher will be the predictive capability of the criterion. The percentage of tests belonging to that I interval (±10%), as related to the total number of tests, vary between 72% for the Findley criterion to 86% for the C&S'. On the other hand, this percentage amounts to 95% for the Papadopoulos criterion. Percentages obtained for all the criteria are presented in Fig. 5, together with those calculated for an I range between -5% and 5%. Again, there is more tests within this range for the Papadopoulos criterion in comparison with all the others.

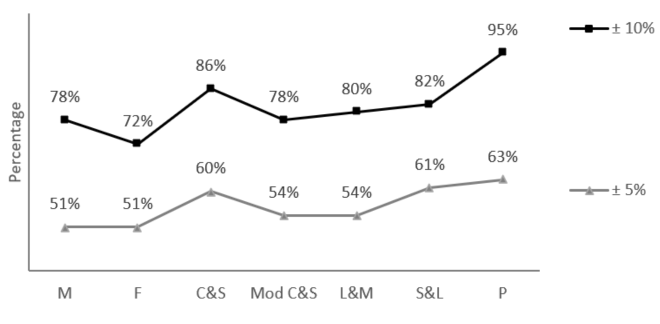

Fig. 5. Percentage of the tests belonging to central I range around 0%.

4. Conclusions

- Dispersion of the error index values associated with applying critical plane-based criteria to a total of 65 cyclic loading conditions varies from one criterion to another. Whereas a dispersion range of 49% is noticed for the L&M criterion, the range displayed by C&S reduces to 36%. Dispersion observed for the other criteria varies between 39% for Findley and 48% for S&L.
- Compared to the critical plane-based criteria, the mesoscopic scale-based model applied to the same loading conditions displays the smallest dispersion range of the error index values.
- Application of the mesoscopic scale-based model is associated with the lowest overall average of the error index values, in comparison with that resulting from the application of any of the critical plane-based criteria.
- The proportion of tests pertaining to a central *I* range around 0% from -10% to 10% amounts to 95% of the total number of tests, a percentage that is higher than that detected for any other of the critical plane-based criteria.

Acknowledgements

This research was developed within the scope of the research and technological development of the Brazilian Electric Energy Sector Program regulated by ANEEL, with the support of the Eneva Companies - Pecém II Energy Generation S.A., Itaqui Energy Generation S.A., Parnaíba Energy Generation and Commercialization S.A. and Parnaíba II Energy Generation S.A.

References

Carpinteri, A., & Spagnoli, A. (2001). Multiaxial high-cycle fatigue criterion for hard metals. *International Journal of Fatigue*, *23*(2), 135–145. https://doi.org/10.1016/S0142-1123(00)00075-X

Carpinteri, A., Spagnoli, A., Vantadori, S., & Bagni, C. (2013). Structural integrity assessment of metallic components under multiaxial fatigue: The C-S criterion and its evolution. *Fatigue and Fracture of Engineering Materials and Structures*, *36*(9), 870–883. https://doi.org/10.1111/ffe.12037

Castro, T. L., Pereira, M. V. S., & Darwish, F. A. (2021). On the Influence of Mean Shear Stress on Multiaxial High Cycle Fatigue of Metallic Materials. *Materials Research*, *24*(1), 20200319. https://doi.org/10.1590/1980-5373-MR-2020-0319

Findley, W. N. (1959). A Theory for the Effect of Mean Stress on Fatigue of Metals Under Combined Torsion and Axial Load or Bending. *Journal of Engineering for Industry*, *81*(4), 301–305. https://doi.org/10.1115/1.4008327

Froustey, C., & Lasserre, S. (1989). Multiaxial fatigue endurance of 30NCD16 steel. *International Journal of Fatigue*. https://doi.org/10.1016/0142-1123(89)90436-2

Liu, Y., & Mahadevan, S. (2005). Multiaxial high-cycle fatigue criterion and life prediction for metals. *International Journal of Fatigue*, *27*(7), 790–800. https://doi.org/10.1016/j.ijfatigue.2005.01.003

Matake, T. (1977). Explanation on Fatigue Limit Under Combined Stress. *Bull JSME*, *20*(141), 257–264. https://doi.org/10.1299/jsme1958.20.257

Nishihara, & Kawamoto. (1945). The Strength of metals under combined alternating bending and torsion with phase difference. *Mem College Eng Kyoto Imp Univ*, *11*, 85–112.

Papadopoulos, I. V., Davoli, P., Gorla, C., Filippini, M., & Bernasconi, A. (1997). A comparative study of multiaxial high-cycle fatigue criteria for metals. *International Journal of Fatigue*, *19*(3), 219–235. https://doi.org/10.1016/S0142-1123(96)00064-3

Susmel, L., & Lazzarin, P. (2002). A bi-parametric Wöhler curve for high cycle multiaxial fatigue assessment. *Fatigue and Fracture of Engineering Materials and Structures*, *25*(1), 63–78. https://doi.org/10.1046/j.1460-2695.2002.00462.x

Wang, Y. Y., & Yao, W. X. (2004). Evaluation and comparison of several multiaxial fatigue criteria. *International Journal of Fatigue*, *26*(1), 17–25. https://doi.org/10.1016/S0142-1123(03)00110-5

Y. S. Garud. (1981). Multiaxial fatigue: a survey of the state-of-the-art. *J Test Eval*, *9*(3), 165–178.

You, B. R., & Lee, S. B. (1996). A critical review on multiaxial fatigue assessments of metals. *International Journal of Fatigue, 18*(4), 235–244. https://doi.org/10.1016/0142-1123(96)00002-3

Zenner, H., Heidenreich, R., & Richter, I. (1985). Dauerschwingfestigkeit bei nichtsynchroner mehrachsiger Beanspruchung. *Materialwissenschaft Und Werkstofftechnik*. https://doi.org/10.1002/mawe.19850160310